Co-simulation based Digital Twin for Thermal Characteristics of Motorized Spindle

Haoran Yi (870894160@qq.com)
University of Shanghai for Science and Technology https://orcid.org/0000-0002-5824-8004
Kaiguo Fan

Research Article

Keywords: Thermal characteristics,Digital twin, BPNN, Co-simulation, Motorized spindle

Posted Date: June 13th, 2022

DOI: https://doi.org/10.21203/rs.3.rs-1719327/v1

Co-simulation based Digital Twin for Thermal Characteristics of Motorized Spindle

Haoran Yi [1]· Kaiguo Fan[1]

School of Mechanical Engineering, University of Shanghai for Science and Technology, Shanghai, China

Abstract:
To improve the accuracy of thermal characteristics analysis of motorized spindle, an on-line correction model of thermal boundary conditions is proposed based on BP neural network (BPNN), the experimental data and simulation results are used to build the BPNN model to correct the thermal boundary conditions of motorized spindle. A digital twin system for thermal characteristics is developed based on the co-simulation of Ansys, Matlab, and LabVIEW to accurately predict the temperature field and thermal deformation of motorized spindle under different working conditions. The experimental results show that the prediction accuracy of temperature field accuracy of the motorized spindle is 98.62%, and the prediction accuracy of thermal deformation is 96.06%, which effectively improves the simulation accuracy of thermal characteristics, and provides the basis for the error compensation and thermal optimization design.

Key words: Thermal characteristics； Digital twin; BPNN; Co-simulation; Motorized spindle

1 Introduction

Intelligent manufacturing closely combines industrialization and informatization, and greatly improves production efficiency and quality [1,2]. As one of the main technologies of intelligent manufacturing, digital twin simulates the behavior of physical entities in real environment with actual production data, Its relationship [3] with the Internet of Things (IoT) and Cyber-Physical System (CPS) as shown in Fig. 1: the physical model of the real world collects data in real time through IoT acquisition system, and then maps it to the virtual world through CPS to reflect the whole life cycle process of the corresponding entity equipment. Liu et al. [4] combined digital twin with finite element method (FEM) and proposed a digital twin-driven approach for traceability and dynamic control of processing quality, which realized the interactive integration of physical workshops and virtual workshops and was applied to the processing of diesel engine connecting rod. Lu [5] et al. combined computer simulation, algorithm analysis and experience evaluation to build a multidimensional digital twin model dedicated to the product life cycle of automobile constant velocity joint. As one of the key technologies of intelligent manufacturing, digital twin has been applied in many fields such as product design and manufacturing. However, the application of digital twin in thermal characteristics of motorized spindle is relatively scarce.

As the core component of high-speed computer numerical control machine tools, the thermal deformation caused by high-speed operation of motorized spindle seriously affects the accuracy of machine tools. Therefore, it is of great significance to accurately analyze the thermal characteristics of motorized spindle. In recent years, many scholars have done a lot of research on thermal characteristics and thermal design of motorized spindle [6], which greatly improve the performance of motorized spindle. Fan et al. [7] used partial least squares (PLS) to predict the thermal deformation of motorized spindle under different working conditions and analyzed the correlation between multiple temperature variables and three-dimensional thermal deformation, which improved the accuracy of the model. Uhlmanna et al. [8] proposed a 3D finite element (FE) prediction model for high precision thermal characteristics of motorized spindle under complex boundary conditions such as heat source, convection and contact. Zhang et al. [9] used the least square to optimize the heat transfer coefficient of the motorized spindle and took the optimized heat transfer coefficient as the boundary of the FE model to improve the accuracy of the temperature rise prediction model of the motorized spindle. Zhang et al. [10] also proposed a method

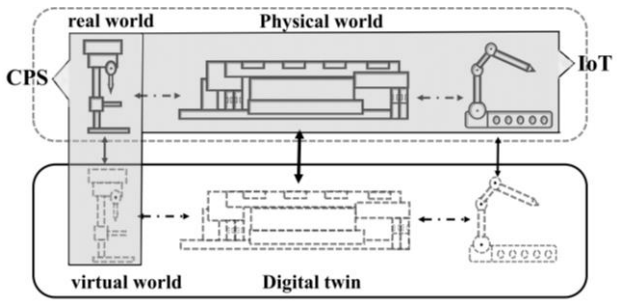

Fig. 1 Relationship between digital twin, CPS, and IoT

✉Kaiguo Fan
Email: fkg11@163.com

Haoran Yi
Email: 870894160@qq.com

for optimizing the heat transfer coefficient based on the biogeography optimization algorithm and develop a thermal deformation prediction model of an intelligent accurate motorized spindle. The developed model is more accurate compared with the conventional thermal deformation prediction model of the motorized spindle.

With the increasing speed of motorized spindle, the analysis and improvement of its thermal characteristics have become a hot spot. At present, the thermal analysis method of motorized spindle is mainly FE thermal simulation. By establishing FE model and applying thermal boundary conditions, the temperature field and thermal deformation of motorized spindle are obtained by FE analysis software. The key is the accurate identification of thermal boundary conditions. Presently, the most typical identification methods include theoretical calculation method [11], experimental measurement method [12], intelligent optimization method [13], and inverse method [14], etc. The existing identification methods can obtain the thermal boundary conditions under specific conditions, which provides a basis for thermal characteristics analysis and thermal optimization design. However, due to the complexity of thermal boundary conditions and experimental limitations, there is a certain deviation between the identification accuracy and the actual value [6]; Furthermore, due to the shape, location and material of the thermal boundary and other factors, it is difficult to determine the exact value [15]. Therefore, it is necessary to carry out in-depth research on accurate identification methods and correction techniques of thermal boundary conditions.

In order to improve the accuracy of thermal analysis of motorized spindle, a modified thermal boundary condition model based on BP neural network (BPNN) is proposed to identify more accurate thermal boundary conditions under different working conditions. The digital twin system of motorized spindle thermal characteristics based on Co-simulation is designed to improve the prediction accuracy of motorized spindle temperature field and thermal deformation.

2 Correction mechanism of thermal boundary condition based on BPNN

2.1 BPNN based correction mechanism for heat generation of bearing

The friction between the bearing rollers and the inner and outer rings during high-speed rotation is the main reason for bearing heat generation [16,17]. The faster the bearing speed is, the more intense the friction is and the greater the heat generation is. In finite element simulation, the bearing roller is usually regarded as the heat source of the bearing, and its heat generation can be calculated according to Palmgren formula and empirical correction formula [16] as,

$$\begin{cases} H_f = \frac{1.047\times10^{-4}n\mathrm{M}}{V_m} \\ M = M_1 + M_2 \\ M_1 = 10^{-7} f_0 (v_0(\Delta t)n)^{\frac{2}{3}} {D_m}^3 \\ M_2 = f_1 P_1(\Delta t) D_m \end{cases} \quad (1)$$

where, H_f is the initial heat generation of the bearing in $\mathrm{W/m^3}$; n is the spindle speed in rpm; M is the bearing friction torque in $\mathrm{N\cdot mm}$, V_m is the bearing volume in $\mathrm{m^3}$; M_1 is the viscous friction torque of lubricating oil; M_2 is the load torque. f_0 is a constant related to bearing type and lubrication mode; $v_0(\Delta t)$ is the kinematic viscosity of lubricating oil changing with temperature in mm^2/s; D_m is the average diameter of the bearing in mm; f_1 is a coefficient related to bearing type and load; $P_1(\Delta t)$ is the bearing load changing with temperature in Newton.

It can be seen from Eq. (1) that for an assembled spindle, the bearing heat generation is proportional to the speed n of the motorized spindle, the bearing load $P_1(\Delta t)$ and the kinematic viscosity of the lubricating oil $v_0(\Delta t)$. Since it is difficult to accurately quantify the bearing load and its size varies with the bearing temperature, it is difficult to accurately calculate the heat generation of the bearing. In order to improve the identification accuracy of bearing heat generation, Reference [16] proposed the correction model of bearing heat generation as,

$$H_f{}' = \frac{t_m - t_\infty}{t_f - t_\infty} \times H_f \quad (2)$$

where, H_f' is the corrected bearing heat in $\mathrm{W/m^3}$; t_m is the measured temperature of the thermal key points in °C; t_f is the finite element analysis temperature of the thermal key points in °C; t_∞ is ambient temperature in °C.

Using Eq. (2), the identification accuracy of heat generation can be improved greatly. In order to further increase the identification accuracy of heat generation, a BPNN based correction method is proposed using the instantaneous temperature rise ratio to further correct the heat generation calculated by Eq. (2). According to the heat transfer theory, if the measured temperature is higher than the simulated temperature, the identified heat generation is less than the actual heat generation of the bearing. According to the relationship between the heat and temperature rise Q=c·m·Δt, the heat flux is proportional to the temperature rise Δt. Therefore, the instantaneous temperature rise ratio is introduced as a correction factor in this study. Take the measured and simulated instantaneous temperature rise ratio as a correction factor of bearing heat generation, the correction function can be established as,

$$\begin{cases} C_H = \Delta t_m / \Delta t_f \\ H_f'' = C_H \times H_f' = f(C_H, H_f') \end{cases} \quad (3)$$

where, C_H is the correction factor; Δt_m and Δt_f are the measured and simulated instantaneous temperature rise, respectively; H_f'' is the bearing heat generation corrected by correction factor in $\mathrm{W/m^3}$.

Due to the nonlinearity of temperature rise, BP neural network is used to predict the heat generation in this study. According to Eqs. (1, 2, 3), the spindle speed, ambient temperature, measured and simulated temperatures at thermal key points of bearing, running time, and initial heat generation can be regarded as the input of neural network; The corrected bearing heat can be regarded as the output of the neural network. According to the analysis abovementioned, the neural network prediction model of front and rear bearing heat generation is composed of a 6-neuron input layer, a 10-neuron hidden layer using the purelin transfer function,

Table 1 Neural network correction sample of heat generation of front bearing at 9000 rpm

Input layer				Output layer
Run time (s)	Measured temperature (℃)	Simulated temperature (℃)	Initial heat generation (W/m^3)	Corrected heat generation (W/m^3)
0	25.34	25.34	1.64×10^6	1.64×10^6
60	28.02	27.66	1.64×10^6	1.723×10^6
120	28.62	28.92	1.64×10^6	1.574×10^6
…	…	…	…	…
1680	31.37	31.31	1.64×10^6	1.667×10^6
1740	31.43	31.25	1.64×10^6	1.679×10^6
1800	31.49	31.46	1.64×10^6	1.642×10^6

and a single output neuron with a logsig transfer function respectively. In order to avoid too small adjustment range of neural network weight and threshold, the elastic gradient descent algorithm (trainrp) is selected to train BP network. Table 1 shows some samples of the heat generation correction of the front bearing of the motorized spindle.

It can be seen from Table 1 that the heat generation of the front bearing changes nonlinearly, which is mainly due to the thermal expansion of the ball during the initial operation of the bearing, resulting in the increase of the bearing load. With the expansion of the inner and outer rings of the bearing, the bearing load gradually decreases, resulting in the decrease of the heat generation. With the expansion of the main shaft, bearing sleeve and other parts, the overall expansion of the bearing also changes continuously. Finally, when the heat balance is reached, the heat generation of the bearing is constant.

2.2 Correction mechanism of thermal contact resistance using neural network

Because the bonding surface is uneven microscopically, that is, the two surfaces are not completely contacted, and the gap between the non-contact interface is filled with medium to form thermal contact resistance [18,19,20]. In ANSYS thermal simulation, it is necessary to accurately define the thermal contact resistance to ensure the accuracy of simulation, so it is necessary to identify the thermal contact resistance through calculation and combined with the correction formula. The initial thermal contact resistance of the bonding surface can be calculated by the following semi-empirical formula as,

$$\frac{r}{Rk} = 105.6\left(\frac{P}{E}\right)^{0.68} \tag{4}$$

where, R is the initial thermal contact resistance in $m^2/K\cdot W$; r is the root mean square roughness in Ra; k is the tuned average thermal conductivity in W/m·K; P is the contact pressure in Mpa; E is the elastic modulus in Gpa.

It can be seen from Eq. (4) that the thermal contact resistance of the bonding surface is proportional to the contact pressure. For the assembled motorized spindle, it is difficult to quantitatively obtain the contact pressure of the bonding surface. Therefore, the correction formula of thermal contact resistance is proposed in Reference [18] as,

$$R' = R\left(1+\left(\frac{P}{EA\left(\sqrt{\frac{1+3\alpha\Delta t}{1+\alpha\Delta t}}-1\right)}\right)^{0.68}\right) \tag{5}$$

where, R' is the corrected thermal contact resistance in $m^2/K\cdot W$; Δt is the temperature change of thermal key points in ℃; α is the coefficient of thermal expansion; A is the area of contact surface in m^2.

According to the heat transfer theory, if the measured temperature is higher than the simulated temperature, the identified thermal contact resistance is greater than the actual value of the bonding surface, and the thermal contact resistance is directly proportional to the interface temperature difference. Therefore, this study introduces a correction factor, that is, the ratio of the measured temperature rise to the simulated temperature rise as a correction factor of the thermal contact resistance, and establishes a correction function as,

$$\begin{cases} C_C = \Delta t_m/\Delta t_f \\ R'' = C_C \times R' = f(C_C, R') \end{cases} \tag{6}$$

where, C_C is the correction factor; R" is the thermal contact resistance corrected by correction factor in $m^2/K\cdot W$.

In Eq. (6), the instantaneous temperature rise is related to the heat generation which is related to the spindle speed. Therefore, the spindle speed, the measured and simulated temperatures of thermal key points, the ambient temperature, the running time, and the initial thermal contact resistance can be regarded as the input of the neural network; The corrected thermal contact resistance can be regarded as the output of the neural network. The thermal contact resistance neural network model is composed of a 6-neuron input layer, a 12-neuron hidden layer and 1-neuron output layer. The transfer function and network training algorithm are consistent with the neural network for predicting bearing heat generation.

2.3 Sample collection and training

The prediction accuracy of neural network depends on the accuracy of samples. The samples of neural network input and output layer in sections 2.1 and 2.2 are obtained by combining experiment, simulation, and calculation. The specific steps are as follows,

The first step is to conduct 20 thermal characteristic tests of motorized spindle running at different speeds for 30 minutes, and store the spindle speed, ambient temperature, and the measured temperature of thermal key points at different running time in the database as part of the samples of input layer.

In the second step, Eqs (1, 4) are applied to calculate the initial heat generation and thermal contact resistance of the motorized spindle as the input layer samples of the neural network.

The third step is to calculate other boundary conditions of thermal characteristic analysis. The heat generation of the motor is calculated by the electromagnetic loss formula, and the convective heat transfer coefficient is calculated by Baz formula.

In the fourth step, the thermal characteristics of the motorized spindle are simulated under the same working conditions as the tests, and the simulated temperatures of thermal key points at the same running time were stored in the database as the input layer samples.

In the fifth step, the measured and simulated temperature of thermal key points are fitted a function of time to calculate the correction parameters of C_H and C_C. Then, the bearing heat generation and thermal contact resistance with correction factors can be calculated by Eqs. (3, 6) as the training samples of output layers of the neural network. The first corrected heat generation H' and thermal contact resistance R' are obtained by online simulation.

To ensure sufficient convergence, the training parameters are set as 5000 epochs, the learning speed is set as 0.05, and the error is set as 10^{-6}, which is calculated by the mean square error function as,

$$MSE = \frac{1}{kp}\sum_{p=1}^{p}\sum_{j=1}^{k}\left(\hat{y}_{kj} - y_{kj}\right)^2 \tag{7}$$

where, k is the number of neurons in the output layer; p is the number of training samples; $\hat{y}_{kj}$ is the expected output of the neural network; y_{kj} is the output of neural network. To improve the training accuracy, the training samples are standardized to the range of (0, 1) through Eq. (8),

$$S = \frac{1}{1+e^{-\sqrt[n]{X}}} \tag{8}$$

where, S is the standardized training sample; X is the initial training samples; n is the maximum order of magnitude of training samples, $n = 6$.

Using Eq. (8) to standardize the training samples of neural network can avoid the problem of computer rounding error and obtain more accurate training results. For the analysis effect of neural network algorithm regression, the R Squared index as shown in Eq. (9) is used, the closer R^2 to 1, the better.

$$\mathrm{R}^2 = 1 - \left(\sum_{\mathrm{i}=0}^{\mathrm{n}} \frac{(\mathrm{Y_i}-\mathrm{O_i})^2}{\sum_{\mathrm{i}=0}^{\mathrm{n}}(\mathrm{Y_i}-\bar{\mathrm{Y}})^2}\right)^2 \tag{9}$$

where, Y is experimental value; O is predictive value. The samples are divided into training set and test set according to the ratio of 8: 2, and the thermal boundary condition correction model is obtained by training. Fig. 2 is the prediction results of partial thermal boundary conditions.

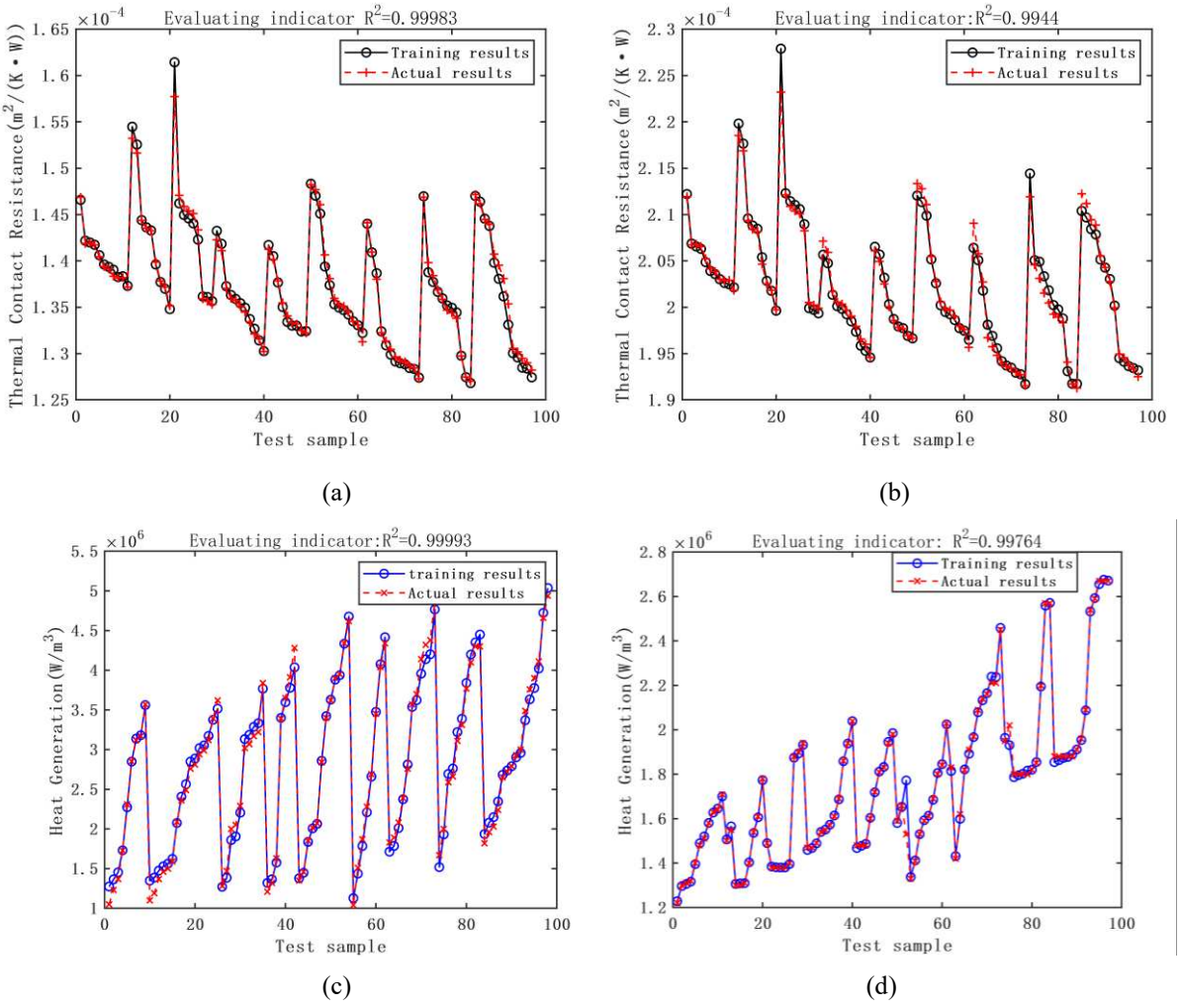

Fig. 2 a: Prediction of thermal contact resistance between front bearing and bearing sleeve
b: Prediction of thermal contact resistance between rear bearing and bearing sleeve
c: Prediction of heat generation of front bearing
d: Prediction of heat generation of rear bearing

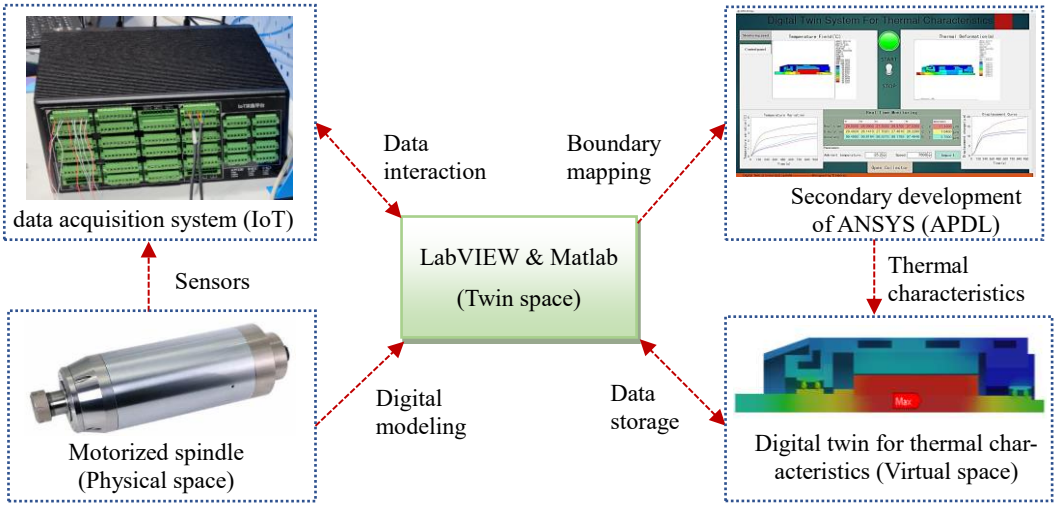

Fig. 3 Digital twin principle of thermal characteristics

It can be seen from Fig. 2 that all the model evaluation indexes are above 0.99. It shows that the prediction effect of thermal boundary conditions of motorized spindle based on BP neural network is good, which can effectively improve the accuracy of finite element analysis.

3 Digital twin for thermal characteristics of motorized spindle

Digital twin is to establish the digital image of the actual physical system in the virtual system, expand new capabilities for the planning and design, state monitoring and motion control of the physical entity, and map the corresponding entity reality through virtual space. As shown in Fig. 3, the digital twin principle of thermal characteristics of motorized spindle is to use the IoT data acquisition system to collect the temperature of thermal key points inside the motorized spindle. After data preprocessing, the thermal boundary conditions are predicted by BP neural network and applied to the virtual model of the motorized spindle. ANSYS Parametric Design Language (APDL) is used to analyze the thermal characteristics of the motorized spindle. The analysis results are mapped to the virtual space to realize the digital twin of the thermal characteristics of the motorized spindle.

3.1 Digital twin system architecture

Fig. 4 shows the architecture of thermal characteristic digital twin system [21]. The digital twin system includes three parts: physical space, twin space and virtual space. The twin space is connected with physical space and virtual space through IoT data acquisition system. Combined with the parameters such as ambient temperature and motorized spindle speed input from the user system interface, the real-time thermal boundary conditions of motorized spindle are predicted through BP neural network and output to APDL command stream file for thermal characteristic simulation of motorized spindle. Finally, the simulation results are mapped to virtual space to realize digital twin of thermal characteristics of motorized spindle.

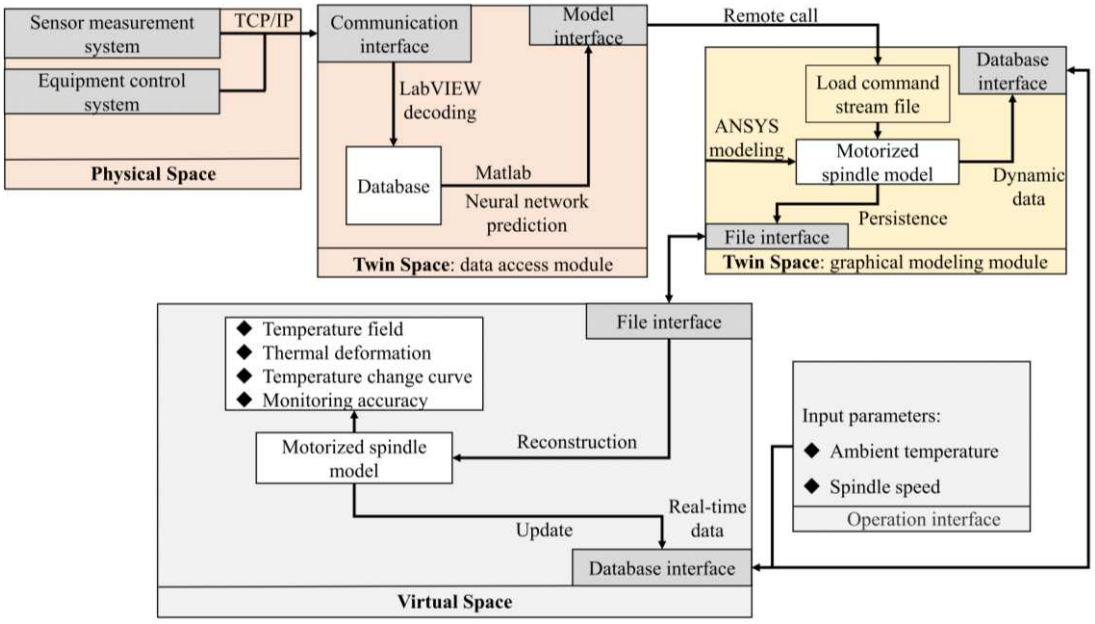

Fig. 4 Framework of digital twin system for thermal characteristics

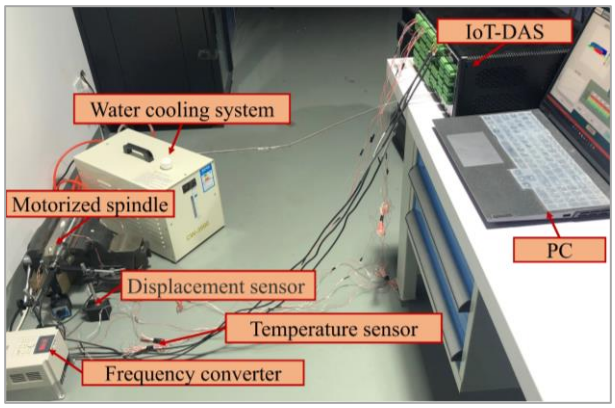

Fig. 5 Physical space of digital twin system

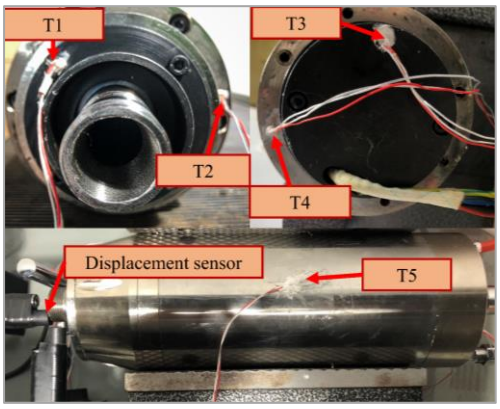

Fig. 6 Layout of sensors for Motorized spindle

3.2 Digital twin system development

3.2.1 Physical space development

The physical space is composed of motorized spindle, sensors, IoT data acquisition system and computer, as shown in Fig. 5. The IoT data acquisition system collects the temperature and displacement data of thermal key points of the motorized spindle measured by the sensors. IoT acquisition system realizes data interaction with host computer database through IP address and port number.

Fig. 6 shows the embedded position of the temperature sensors in the motorized spindle. Five temperature sensors are used to measure the temperature of thermal key points during motorized spindle running [22], in which T1 and T2 are installed at the front bearing outer ring and front bearing sleeve to measure the temperature of the front bearing outer ring and bearing sleeve; T3 and T4 are installed at the rear bearing outer ring and rear bearing sleeve to measure the temperature of the rear bearing outer ring and bearing sleeve; T5 is pasted on the motorized spindle housing to measure the temperature of the motorized spindle shell. The data collected by each temperature sensor is used to realize the real-time correction of the thermal boundary conditions of the motorized spindle.

3.2.2 Twin space development

Twin space mainly includes data access module and graphic modeling module [23]. The data access module is mainly the data interaction between MATLAB, LabVIEW and IoT data acquisition system. The communication software based on TCP / IP protocol is developed by using LabVIEW to import the experimental data into the database in real time. Then, combined with the ambient temperature and motorized spindle speed input by the user in the graphical interface as the input layer of the neural network model, the real-time thermal boundary conditions of motorized spindle are predicted through remote call of Matlab. The specific communication flow of TCP is shown in Fig. 7.

The client and the server realize information transmission through sockets. After the connection is established, the server analyzes the request message according to the protocol specification after receiving the request message, and then returns the response message to the client to obtain real-time data.

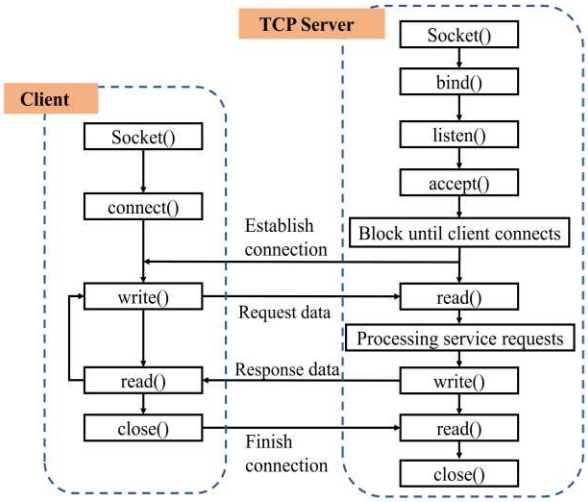

Fig. 7 TCP communication flow

The graphical modeling module is mainly the data interaction between Matlab GUI and APDL command stream file. Due to the use of ANSYS for thermal characteristics simulation analysis requires a certain amount of calculation time, in order to avoid mutual error, the predicted thermal boundary conditions are transmitted to the APDL command stream file every 60 seconds for Ansys batch start-up for thermal-structural coupling simulation. The APDL post-processing content includes the export of motorized spindle temperature field, thermal deformation field, simulation temperature of thermal key points, correction data, etc. The post-processing results are saved to the database, where the simulation temperature of thermal key points and the running time of motorized spindle are called to the neural network model as the input layer. The specific data interaction process of twin space is shown in Fig. 8.

3.2.3 Virtual space development

As shown in Fig. 9, a digital twin system based on Matlab GUI, APDL and LabVIEW is developed to study the thermal characteristics of motorized spindle. The application can realize the starting, stopping, and speed change of motorized spindle, real-time data interaction, result visualization, monitoring correction accuracy and, etc.

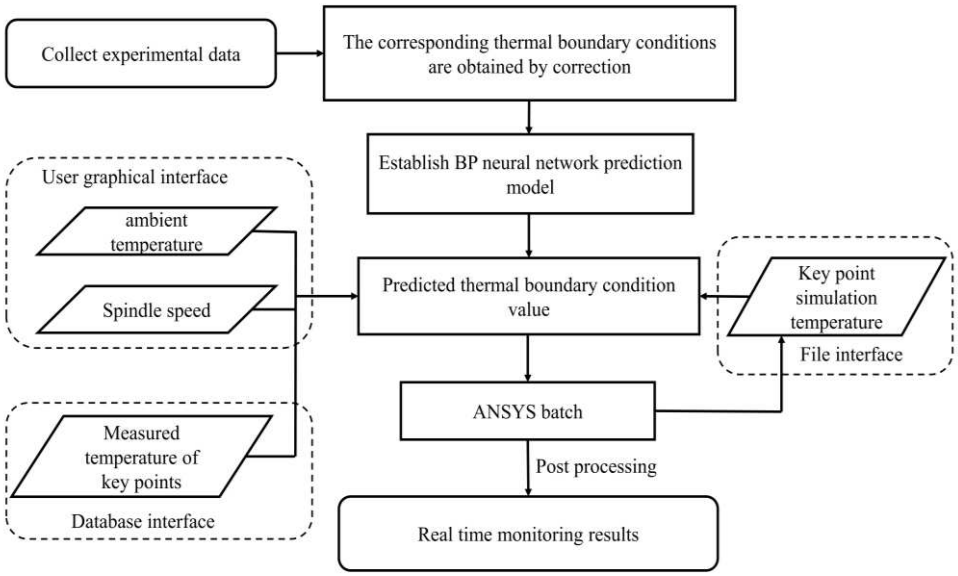

Fig. 8 Data interaction flow of twin space

In the system interface, the user only needs to input the ambient temperature and motorized spindle speed. In the background, the input parameters are transmitted to the twin space every 60 seconds through the I/O flow to complete the transient thermal-structure coupling simulation with a step length of 4 seconds and a step end time of 60 seconds, and then the simulated temperature field and thermal deformation of the motorized spindle are displayed in real time through UIAxes component in Matlab GUI. The real-time temperature of the five key points, the thermal deformation of the core spindle along X-, Y-, and Z-directions, and the monitoring accuracy are displayed in real time through the UITable component. Finally, the historical data is stored in the database to provide a basis for error compensation and thermal optimization design.

4 Experimental validation

For a type of high-speed motorized spindle, the physical space is arranged as shown in Figs. 5 and 6, and the thermal characteristics of the motorized spindle running at the speed as shown in Table 2 for 30 minutes are tested by using the thermal characteristics digital twin system. Three eddy current displacement sensors are used to measure the thermal deformation of core spindle along the X-, Y-, and Z-directions, and the laboratory temperature was 25.34 °C. Fig. 10 shows the digital twin diagram of thermal characteristics of motorized spindle when it runs at 9000r/min for 30 minutes.

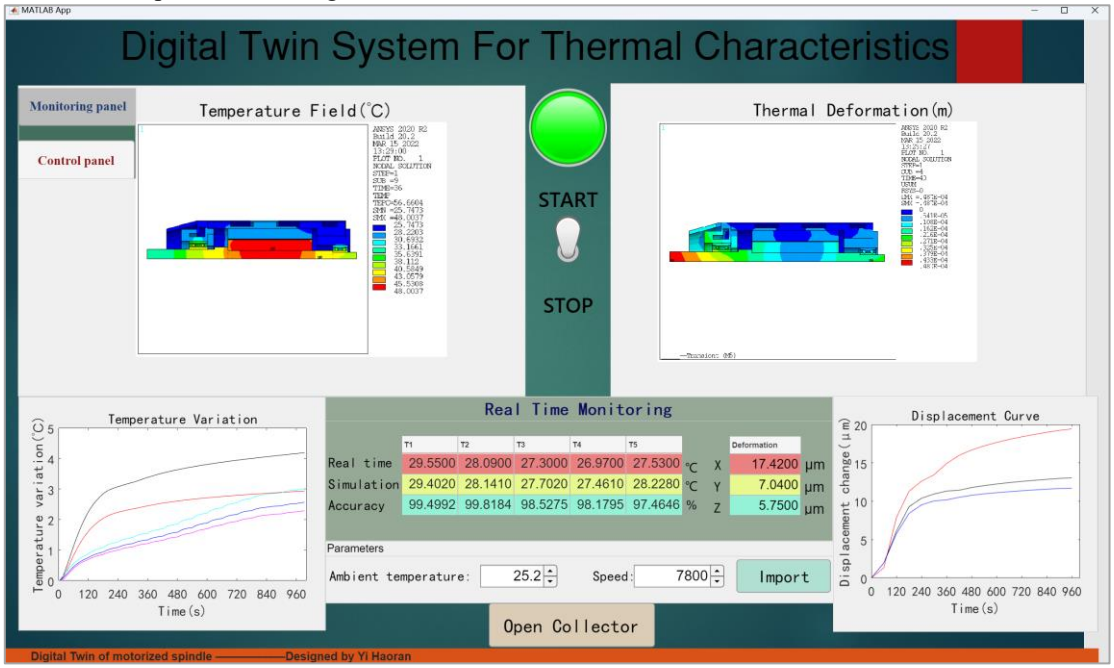

Fig. 9 User interface of digital twin system

Table 2 Monitoring accuracy under different rotating speed and temperature environment

Speed (rpm)	Ambient temp. (℃)	Temp. accuracy (%)	Thermal deformation accuracy (%)	Average accuracy (%)	
7200	24.49	99.3	95.6	Temp.	Deformation
8400	24.90	98.8	96.2		
9000	25.34	99.6	96.5		
9600	25.50	98.5	97.1		
10200	25.17	98.7	95.4	98.62	96.06
11400	24.50	99.2	95.6		
12000	23.90	98.9	96.2		
12600	24.62	99.1	95.9		

Fig. 10 (a) shows the temperature field of the motorized spindle. The areas with high temperature of the motorized spindle are concentrated at the front and rear bearings, stator, and rotor, of which the rotor temperature is the highest which is 57.017 ℃, followed by the front and rear bearings and stator. The main reason is that the bearings and stator are assembled inside the spindle and the heat dissipation conditions are poor, but part of the heat of the front and rear bearings and stator is transferred to the cooling system and taken away by the coolant, while the rotor can only dissipate heat through internal air convection and radiation. Fig. 10 (a) also shows that the temperature field of the motorized spindle is ununiform, which will lead to inconsistent thermal deformation of the components and thus affect the thermal boundary conditions. Fig. 10 (b) shows the thermal deformation of the motorized spindle, and the maximum thermal deformation is 8.47 μm which occurs at the front end of the core spindle.

Fig. 11 shows the comparison of thermal characteristics between digital twin and actual measurement results at the speeds of 7800 rpm and 10800 rpm. It can be seen from Fig. 11 that the digital twin of thermal characteristic based on neural network correction of thermal boundary can better map the thermal characteristic of the motorized spindle, and can realize the whole process mapping of thermal characteristic of the motorized spindle, and have good following performance.

Table 2 shows the digital twin accuracy of thermal characteristics of motorized spindle under different test speeds. Among them, the minimum accuracy of five key temperature measurement points is 98.5%, and the average accuracy is 98.62%; The minimum accuracy of thermal deformation is 95.4%, and the average accuracy is 96.06%. It proves that the digital twin for thermal characteristics of motorized spindle based on BP neural network can effectively improve the accuracy of thermal characteristic analysis of motorized spindle.

Based on the comprehensive analysis of the digital twin results of the thermal characteristics of the motorized spindle, the following performance needs to be improved when the temperature rise rate of the motorized spindle changes rapidly. As shown in Fig. 11, the temperature accuracy of the key temperature measurement point T2 near 200 seconds is lower than at other times due to the fact that the neural network training samples are collected at evenly distributed time intervals, while the temperature rise rate changes rapidly when it tends to thermal equilibrium. The prediction accuracy can be improved by increasing the collected samples in this time period.

5. Conclusion

Accurate thermal characteristic analysis of motorized spindle is the premise of thermal optimization design and error compensation. Due to the complexity of boundary conditions, the accuracy of thermal characteristic analysis of motorized spindle is limited. In order to improve the accuracy of thermal characteristic analysis, the correction model of thermal contact resistance of joint surface and bearing heat generation is constructed based on BP neural network, and the digital twin system for thermal characteristics of motorized spindle is developed based on ANSYS, MATLAB and LabVIEW to realize the digital twin for thermal characteristics of motorized spindle. According to the test results, the following conclusions are drawn.

The training accuracy of BP neural network is highly related to the samples. The samples of the input layer can be accurately obtained by sensors, while the samples of the output layer need to be obtained by combining test, simulation and correction function. Constructing an accurate correction function can effectively improve the prediction accuracy of neural network; The collection of training samples also has a great impact on the training accuracy of the network. The sample collection volume can be increased in the area with large changes in thermal characteristics to improve the prediction accuracy. The test results show that the accuracy of digital twin temperature and thermal deformation of motorized spindle based on BP neural network correcting thermal boundary conditions is 98.62% and 96.06%, which can effectively improve the accuracy of finite element analysis of thermal characteristics, and lay a foundation for error compensation and performance optimization of motorized spindle.

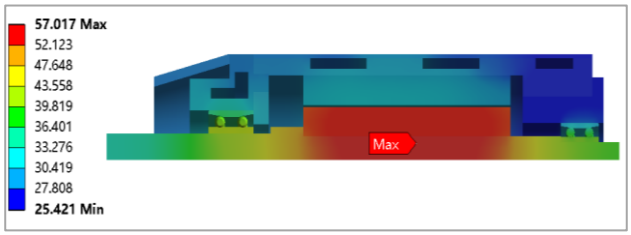

(a)

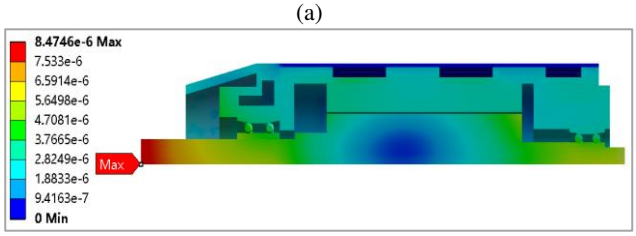

(b)

Fig. 10 **a**: Temperature field
b: Thermal deformation

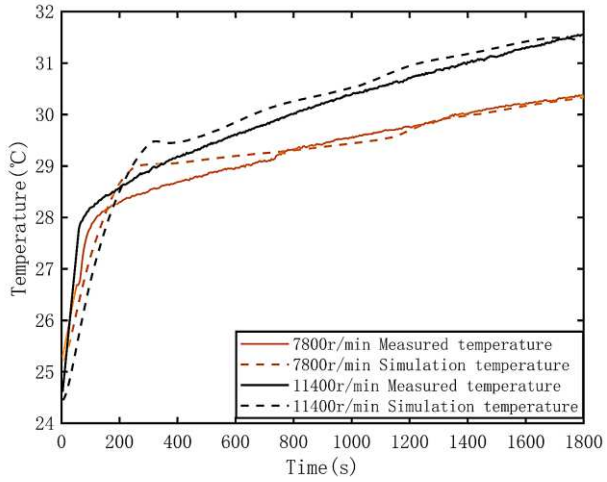

(a) Temperature rise at thermal key point T1

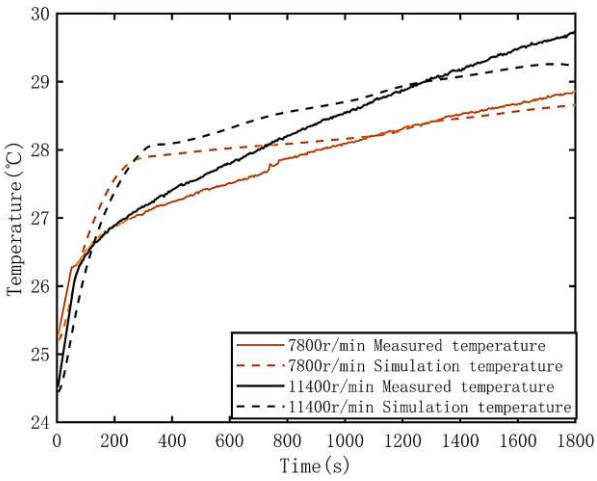

(b) Temperature rise at thermal key point T2

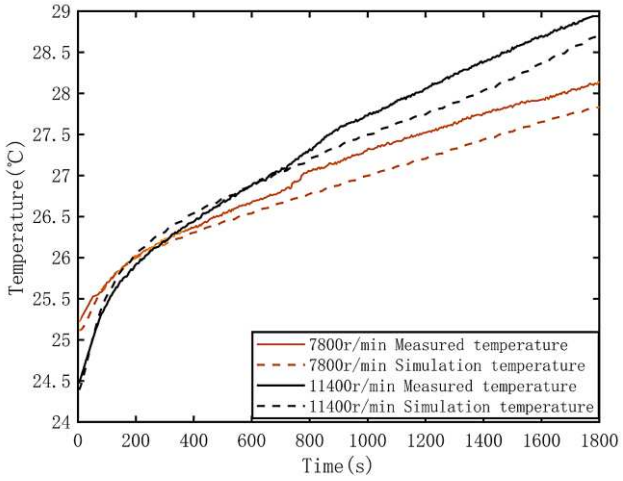

(c) Temperature rise at thermal key point T3

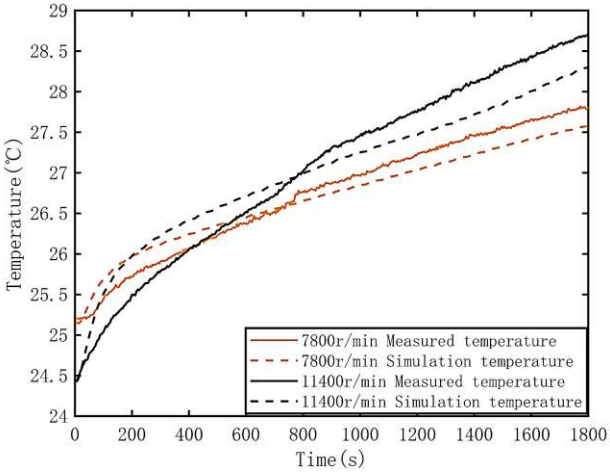

(d) Temperature rise at thermal key point T4

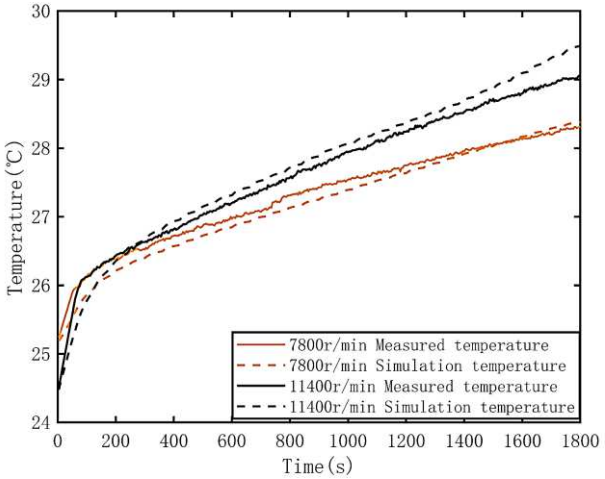

(e) Temperature rise at thermal key point T5

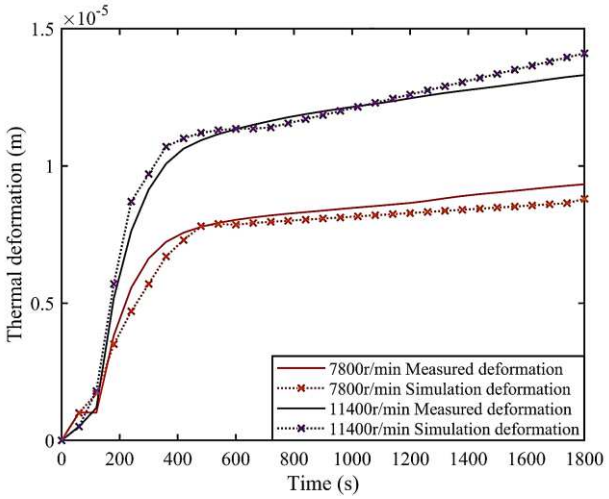

(f) Thermal deformation of core spindle

Fig. 11 Comparison of thermal characteristics between digital twin and actual measurement results

Declarations

a. Funding: the authors declare that no funds, grants, or other support were received during the preparation of this manuscript.
b. Competing Interests: the authors have no relevant financial or non-financial interests to disclose

c. Availability of data and material: all data generated or material during this study are included in this published article.
d. Code availability: all the Matlab, APDL, LabView code are available
e. Ethics approval: the authors confirm that this work is an original work and has not been published in other places, and all the data is true.
f. Consent to participate: the authors consent to participate.

g. Consent for publication: the authors consent to publish the paper.

h. Authors' contributions： Fan pointed out the research direction and the feasibility of the experiment. Yi operated all the experiments, programmed and wrote the manuscript. Fan finally polished the manuscript.

References

1. Wu Y, Wang XJ, He Y, Huang XW, Xiao LJ, Guo LX (2021) Review on the technology and application of digital twin in manufacturing industry. Modern Manufacturing Engineering 09: 137-145. https://doi.org/10.16731/j.cnki.1671-3133.2021.09.023
2. Li H, Wang HQ, Liu G, Wang JL, Evans S, Li LL, Wang XC, Zhang S, Wen XY, Lie FQ, Wang XC, Hao B, Jiang W, Liu YG (2021) Concept, system structure and operation mode of industrial digital twin system. Comput. Integr. Manuf. Syst 27(12): 3373-3390. https://doi.org/10.13196/j.cims.2021.12.001
3. Miao T, Zhang X, Xiong H, Zhuang CB, Zhao HR, Lv Z (2019) Liu, J.H.: Application and expectation of digital twin in product lifecycle. Comput. Integr. Manuf 25(6): 1546-1558. https://doi.org/10.13196/j.cims.2019.06.022.
4. Liu JF, Cao XW, Zhou HG, Li L, Liu XJ, Zhao P, Dong JW (2021) A digital twin-driven approach towards traceability and dynamic control for processing quality. Adv. Eng. Inform 50:101395. https://doi.org/10.1016/j.aei.2021.101395
5. Lu YJ, Zhao ZC, Wang W, Zhang K (2021) Digital twin product lifecycle system dedicated to the constant velocity joint. Comp. Elec. Engi 93: 107264. https://doi.org/10.1016/j.compeleceng.2021.107264
6. Deng XL, Lin H, Wang JC, Xie CX, Fu JZ (2018) Review on thermal design of machine tool spindles. Opt. Precision Eng 26(06): 1415-1429. https://doi.org/10.3788/OPE.20182606.1415
7. Fan LT, Jing XR, Zhang K, Zhu CX (2020)Thermal Deformation Modeling and Analysis of High Speed Motorized Spindle Based on PLS. Journal of Shenyang Jianzhu University (Natural Science) 36(04): 738-744. https://doi.org/10.11717/j.issn:2095-1922.2020.04.20
8. Uhlmann E, Hu J (2012) Thermal modelling of a high speed motor spindle. Procedia CIRP. 1: 313-318: https://doi.org/10.1016/j.procir.2012.04.056
9. Zhang LX, Li CQ, Li JP, Zhang K, Wu YH (2017) The Temperature Prediction Mode of High Speed and High Precision Motorized Spindle. J. Mech. Eng 53(23): 129-136. https://doi.org/10.3901/JME.2017.23.129
10. Zhang LX, Gong WJ, Zhang K, Wu YH, An D, Shi HT, Shi QH (2018) Thermal deformation prediction of high-speed motorized spindle based, Int. J. Adv. Manuf. Technol 97:3141–3151. https://doi.org/10.1007/s00170-018-2123-6
11. Song S, Yovanvich MM (1988) Relative contact pressure - Dependence on surface roughness and Vickers microhardness. Journal of Thermophysics and Heat Transfer 2(1): 43-47. https://doi.org/10.2514/3.60
12. Ishizaki T, Igami T, Nagano H (2020) Measurement of local thermal contact resistance with a periodic heating method using microscale lock-in thermography. Rev. Sci. Instrum 91(6): 0640901. https://doi.org/10.1063/5.0002937
13. Tan F, Yin Q, Dong GH, Xie LF, Yin GF (2017) An optimal convective heat transfer coefficient calculation method in thermal analysis of spindle system. Int. J. Adv. Manuf. Technol 91(5): 2549-2560. https://doi.org/10.1007/s00170-016-9924-2
14. Yu YF, Li ZW, Zheng XY (2018) The inverse problem of thermal contact resistance between rough surfaces. Chinese Journal of Theoretical and Applied Mechanics 50(3): 479-486. https://doi.org/10.6052/0459-1879-18-076
15. Li HL, Ying XJ (2010) A Design Method of Temperature Measurement Points for Thermal Error of Machine Spindle. China Mechanical Engineering 21(07):804-808.
16. Fan KG (2017) Research on the Machine Tool's Temperature Spectrum and Its Application in a Gear form Grinding Machine. Int. J. Mach. Tools Manuf 90: 3841-3850. https://doi.org/10.1007/s00170-016-9722-x
17. Sathiya Moorthy R, Prabhu Raja V (2014) An Improved Analytical Model for Prediction of Heat Generation in Angular Contact Ball Bearing. Arab. J. Sci. Eng 39: 8111–8119. https://doi.org/10.1007/s13369-014-1351-9
18. Fan KG, Gao R, Zhou H, Le W, Shen RJ, Xu Y, Zhao Y, Lu QJ, Wang RD, Li YF (2018) Study on the on-line correction of thermal parameters for machine tools. Mechanical Engineering and Technology 7(06): 480-486. https://doi.org/10.12677/MET.2018.76059
19. Beriache M, Bettahar A, Naji H, Loukarfi L, Mokhtar Saïdia L (2012) Fluid Flow and Thermal Characteristics of a Minichannel Heat Sink with Impinging Air Flow. Arab. J. Sci. Eng 37: 2243–2254. https://doi.org/10.1007/s13369-012-0321-3
20. Fang B, Cheng MN, Gu TQ, Ye DP (2022) An improved thermal performance modeling for high-speed spindle of machine tool based on thermal contact resistance analysis. Int. J. Adv. Manuf. Technol 120: 5259–5268. https://doi.org/10.1007/s00170-022-09085-4
21. Yan ZZ, Tao T, Hou RS, Du HY, Mei XS (2020) A new modeling method for thermal errors of motorized spindle based on the variation characteristics of spindle temperature field. Int. J. Adv. Manuf. Technol 110:989–1000. https://doi.org/10.1007/s00170-020-05752-6
22. Liu YC, Miao EM, Zhang MD, Feng D, Li JG (2021) Selection of robust temperature-sensitive points for CNC machine tools. Opt. Precision. Eng 29(05):1072-1083. https://doi.org/10. 37188/OPE.20212905.1072
23. Prabhu Raja V, Sathiya Moorthy R (2019) Prediction of Temperature Distribution of the Spindle System by Proposed Finite Volume and Element Method. Arab. J. Sci. Eng 44: 5779–5785. https://doi.org/10.1007/s13369-019-03732-x